Why Does the Reaction of the Dihydrogen Molecule with $[P_2N_2]Zr(\mu\text{-}\eta^2\text{-}N_2)Zr[P_2N_2]$ Produce $[P_2N_2]Zr(\mu\text{-}\eta^2\text{-}N_2H)Zr[P_2N_2](\mu\text{-}H)$ but Not the Thermodynamically More Favorable $[P_2N_2]Zr(\mu\text{-}NH)_2Zr[P_2N_2]$? A Theoretical Study

Harold Basch,*,† Djamaladdin G. Musaev,* and Keiji Morokuma*

Contribution from the Cherry L. Emerson Center for Scientific Computation and the Department of Chemistry, Emory University, Atlanta, Georgia 30322

Received December 22, 1998. Revised Manuscript Received April 27, 1999

Abstract: The mechanism of reaction of binuclear zirconium dinitrogen complex $[p_2n_2]Zr(\mu\text{-}\eta^2\text{-}N_2)Zr[p_2n_2]$ (**1**, where $p_2n_2 = (PH_3)_2(NH_2)_2$ as a model of the experimentally used $P_2N_2 = PhP(CH_2SiMe_2NSiMe_2CH_2)_2$-PPh ligand), with a hydrogen molecule has been studied by using the density functional method. It is shown that this reaction proceeds via (i) activation of the H−H σ-bond via a "metathesis-like" transition state where simultaneously Zr−H and N−H bonds are formed and the H−H and one of the N−N π-bonds are broken, to produce the diazenidohydride complex **3**, $[p_2n_2]Zr(\mu\text{-}\eta^2\text{-}NNH)Zr(H)[p_2n_2]$, and (ii) migration of the Zr-bonded hydride ligand to a position bridging the two Zr atoms to form the diazenido−μ-hydride complex **7**, $[p_2n_2]Zr(\mu\text{-}\eta^2\text{-}NNH)Zr[p_2n_2](\mu\text{-}H)$. The entire reaction is calculated to be exothermic by 13−15 kcal/mol. The rate-determining step of this reaction is found to be the activation of the H−H bond, which occurs with a 21-kcal/mol barrier. The experimentally observed diazenido−μ-hydride complex **7**, $[p_2n_2]Zr(\mu\text{-}\eta^2\text{-}NNH)Zr[p_2n_2](\mu\text{-}H)$, is not the lowest energy structure in the potential energy surface. The hydrazono complex $[p_2n_2]Zr(\mu\text{-}NNH_2)Zr[p_2n_2]$ (with a bridging NH_2) and the hydrado complex $[p_2n_2]Zr(\mu\text{-}NHNH)Zr[p_2n_2]$ (with two bridging NH units) are calculated to be more stable than the diazenido−μ-hydride complex **7** by about 50 kcal/mol. However, these complexes cannot be generated by the reaction of **1** + H_2 at ambient laboratory conditions because of very high (nearly 60 kcal/mol) barriers separating them from **7**.

1. Introduction

Activation of the N≡N triple bond and its chemical transformations has attracted great interest from both fundamental and practical points of view.[1−7] Perhaps the most famous and oldest such reactions is the energy-intensive Haber−Bosch process,[1,2] which annually accounts for the production of millions of tons of ammonia directly from dinitrogen and dihydrogen molecules with use of an iron metal catalyst. The biological analogue to this industrial process appears to be the nitrogenase process.[3] Extensive attempts to find the new processes better than Haber−Bosch and nitrogenase processes have not met with success, although they have led to the discovery of several important reactions which are believed also to occur in these processes.

The first of these is a catalytic cleavage of the N≡N triple bond by transition metal complexes.[5] The cleavage of the N≡N triple bond of the bare N_2 molecule is not easy because of its very high binding energy (D_e = 225.94 ± 0.14 kcal/mol), reflected in its short N≡N equilibrium distance (R_e = 1.0976 Å).[8] Although some highly reducing systems, such as a mixture of a metal−halide with an excess of a Grignard reagent, that react with N_2 to form nitrides have been recognized for many years,[2f] the clean splitting of the N≡N triple bond has only recently been achieved by Cummins with a tridentate amine complex of Mo, $Mo(NRAr)_3$, where R = $C(CH_3)_2CH_3$ and Ar = 3,5-$C_6H_3Me_2$.

The second is the reaction of a coordinated N_2 molecule with electrophiles (protons, organic free radicals, acidic transition metal complexes, or a coordinated H_2 molecule) via protonation,[2g,6] and with molecular hydrogen via hydrogenation by Fryzuk et al.[7] Since a metal-coordinated N_2 presumably already

† On sabbatical leave from the Department of Chemistry, Bar Ilan University, Ramat Gan, Israel.

(1) Jennings, J. R., Ed. *Catalytic Ammonia Synthesis*; Plenum: New York, 1991.

(2) (a) Ludden, P. W. *Encyclopedia of Inorganic Chemistry*; Wiley: New York, 1994; p 2566. (b) Coucouvanis, D. *Encyclopedia of Inorganic Chemistry*; Wiley: New York, 1994; p 2557. (c) Howard, J. B.; Rees, D. C. *Chem. Rev.* **1996**, *96*, 2965. (d) Burgess, B. K.; Lowe, D. J. *Chem. Rev.* **1996**, *96*, 2983. (e) Eady, R. R. *Chem. Rev.* **1996**, *96*, 3013. (f) Leigh, G. J. *Science* **1998**, *279*, 506. (g) Leigh, G. J. *Acc. Chem. Res.* **1992**, *25*, 177 and references therein.

(3) Eady, R. R. *Perspectives on Bioinorganic Chem*istry; JAI Press: Greenwich, CT, 1991; p 255.

(4) (a) Kim, J.; Rees, D. C. *Science* **1992**, 257, 1667. (b) Kim, J.; Rees, D. C. *Nature* **1992**, *360*, 553. (c) Chan, M. K.; Kim, J.; Rees, D. C. *Science* **1993**, *260*, 792. (d) Demadis, K. D.; Coucouvanis, D. *Inorg. Chem.* **1995**, *34*, 436. (e) Malinak, S. M.; Simeonov, A. M.; Mosier, P. E.; McKenna, C. E.; Coucouvanis, D. *J. Am. Chem. Soc.* **1997**, *119*, 1662 and references therein.

(5) (a) Laplaza, C. E.; Cummins, C. C. *Science* **1995**, *268*, 861. (b) Laplaza, C. E.; Odom, A. L.; Davis, W. M.; Cummins, C. C. *J. Am. Chem. Soc.* **1995**, *117*, 4999. (c) Odom, A. L.; Cummins, C. C. *J. Am. Chem. Soc.* **1995**, *117*, 6613. (d) Laplaza, C. E.; Johnson, A. R.; Cummins, C. C. *J. Am. Chem. Soc.* **1996**, *118*, 709. (e) Laplaza, C. E.; Johnson, M. J. A.; Peters, J. C.; Odom, A. L.; Kim, E.; Cummins, C. C.; George, G. N.; Pickering, I. J. *J. Am. Chem. Soc.* **1996**, *118*, 8623.

(6) Nishibayashi, Y.; Iwai, S.; Hidai, M. *Science* **1998**, *279*, 540.

(7) Fryzuk, M. D.; Love, J. B.; Rettig, S. J.; Young, V. G. *Science* **1997**, *275*, 1445.

(8) *CRC Handbook of Chemistry and Physics*, 72nd ed.; CRC Press: Boca Raton, Ann Arbor, and Boston, 1991−1992.

10.1021/ja984408w CCC: $18.00
Published on Web 06/03/1999

has an activated N−N bond, it is expected to react with molecular hydrogen (and other hydrides) more easily than the bare N_2 molecule.

However, the mechanisms of these nitrogen-activation and transformation processes are not well understood, and their detailed understanding is highly desirable. In previous papers we have studied the mechanism of N_2 cleavage by three-coordinate group 6 complexes ML_3 (where M = Mo and W and L = Cl, NH_2, and OCH_3) in detail.[9] It has been shown that this reaction is a multistep process including (i) coordination of the dinitrogen molecule to the transition metal center of the quartet ground state of the ML_3 complex to form a doublet (N_2)-ML_3 intermediate, (ii) coordination of the second ML_3 fragment to form a stable triplet binuclear complex, $L_3M(N_2)ML_3$, (iii) crossover from the triplet to the singlet state, and (iv) N−N cleavage over a significant barrier to form two NML_3 complexes. The barrier to N−N bond cleavage can be controlled by the number and the kind of ligands L and the metal M. Strongly π-donating ligands L decrease the barrier; the NRAr ligand used experimentally[5] was the best choice. Calculations[9] also suggest that WL_3 is more active than MoL_3.

In the present paper, which is a continuation of previous theoretical studies of the cleavage of the coordinated N_2,[9] we will present the results of theoretical studies of the mechanism of reaction of a H_2 molecule with a dinitrogen molecule coordinated to two Zr complexes, experimentally reported by Fryzuk and co-workers.[7] Previously, this group had reported[10] on the synthesis and spectroscopic characterization of various binuclear M−N_2−M complexes involving both the end-on μ^1-N_2 and the side-on μ^2-N_2 bonding mode. The only experimentally determined end-on structure is found to have a shorter N−N bond length of 1.30 Å, while the side-on forms have unusually long N−N bond lengths of 1.55−1.43 Å. The composition of the auxiliary ligands seems to determine whether the side-on or end-on complex is formed. Furthermore, even for a given orientation type of the complex, the N−N bond distance (which should reflect the degree of N≡N bond activation) is sensitive to the nature of the exterior ligands, giving the range of N−N distances quoted above.

The novel aspect of Fryzuk et al.'s latest report[7] is the ability of $[P_2N_2]Zr(\mu\text{-}\eta^2\text{-}N_2)Zr[P_2N_2]$ (**I**, where P_2N_2 = $PhP(CH_2SiMe_2NSiMe_2CH_2)_2PPh$) to react with molecular hydrogen to form $[P_2N_2]Zr(\mu\text{-}\eta^2\text{-}N_2H)Zr[P_2N_2](\mu\text{-}H)$ (**II**) containing an N−H bond on the bridging N_2 molecule and a metal bridging hydride. This is the first example of the reaction of a coordinated N_2 molecule with molecular hydrogen. Although the N−N bond is not split in this reaction, product **II** could be an intermediate in the process of obtaining ammonia directly from N_2 and H_2 at ambient conditions. Our recent joint paper, based on the density functional calculations for a simplified model of **I** (called **1** later) using the ligand $[p_2n_2] = (PH_3)_2(NH_2)_2$ and neutron diffraction/inelastic scattering studies,[11] confirms that the product of the reaction **I** + H_2 is the $(\mu\text{-}\eta^2\text{-}N_2H)(\mu\text{-}H)$ complex **II** proposed from the solution data,[7] rather than the $(\mu\text{-}\eta^2\text{-}N_2)(\mu\text{-}\eta^2\text{-}H_2)$ complex **III** from the low-temperature X-ray study.[7] This same study[11] also reported the analogous geometric structures calculated for the bridging metal complexes resulting from the reaction of **1** with CH_4 and SiH_4 molecules. Note that the reaction of **I** with primary silanes $RSiH_3$ was also studied experimentally[7] with the resulting formation of only one product, $[P_2N_2]Zr(\mu\text{-}\eta^2\text{-}N_2SiH_2R)Zr[P_2N_2](\mu\text{-H})$. On the basis of the comparison of the calculated energetics for the reactions of **1** with H_2, CH_4, and SiH_4, it was concluded that **I** can activate the H−H and Si−H bonds of dihydrogen and primary silanes, respectively, but not the C−H bond of alkanes.

However, these novel experimental studies[7,11] and previous calculations[11] left several key questions unanswered about the mechanism of the reaction of **I** with H_2. In the present paper we will report on the calculations and address some of these questions; namely, (1) what is a mechanism of the reaction of **I** with H_2, and (2) what are the structures and energies of all the equilibrium, intermediates, and transition states on the reaction path of **I** + H_2? Also, we will very briefly discuss the role of the auxiliary ligands of $[P_2N_2]$. A detailed discussion on the effects of the different external ligands, together with studies on the effects of different metals, and the possibility of successive reactions of complex **I** with more than one hydrogen molecule will be presented in a subsequent paper.[12]

The electronic and geometrical structural properties of bare MN_2M complexes have been the subject of several theoretical studies.[13] In general, it was shown that the side-on coordinated MN_2M systems may have two different low-lying electronic states. The first of them is characterized by a high-spin state and an intermediately perturbed N_2 unit with an N−N distance close to the double bond in azomethane (1.24 Å). The second state is characterized by a low-spin state and a strongly perturbed N_2 unit with an N−N distance close to the single bond in hydrazine (1.47 Å). The low-spin state is the ground state for the second-row metals to the left in the periodic table (Y and Zr), while the high-spin state is lower in energy for the second-row metals to the right of Zr and for all first-row metals. On the basis of comparison of the calculated geometries for the naked ZrN_2Zr system with those for the experimentally studied systems such as **I**, it was concluded that the auxiliary ligands on the metal atoms have a very small influence on the electronic and geometrical structure of the central Zr_2N_2 unit. All calculated bare side-on MN_2M (M = Ti, Y, and Zr) complexes are calculated to have a planar structure.

2. Computational Procedure

Since it is technically impossible to explicitly compute the potential energy surface of the reaction **I** + H_2 for the experimentally used complex **I** with the $[P_2N_2]$ = $PhP(CH_2SiMe_2NSiMe_2CH_2)_2PPh$ tetradentate ligand at a reasonably high level of the theory, some kind of modeling of the complexes and reaction is needed. However, one should be aware that unreasonable modeling may lead to unrealistic results, therefore, we should be extremely careful. Here, as in our previous computational study[11] of the structures and energetics of the reaction of **I** with H_2, CH_4, and SiH_4, each $[P_2N_2]$ = $PhP(CH_2SiMe_2NSiMe_2CH_2)_2PPh$ tetradentate ligand in the real complex was replaced by $[p_2n_2] = (PH_3)_2(NH_2)_2$ in the model compound. In other words, the coordinated phosphine and nitrogen atoms of the tetradentate macrocyclic $[P_2N_2]$

(9) (a) Cui, Q.; Musaev, D. G.; Svensson, M.; Sieber, S.; Morokuma, K. *J. Am. Chem. Soc.* **1995**, *117*, 12366. (b) Musaev, D. G.; Cui, Q.; Svensson, M.; Morokuma, K. In *Transition State Modeling for Catalysis*; Truhlar, D. G., Morokuma, K., Eds.; American Chemical Society, Washington, 1998.

(10) (a) Fryzuk, M. D.; Haddad, T. S.; Rettig, S. J. *J. Am. Chem. Soc.* **1990**, *112*, 8185. (b) Fryzuk, M. D.; Haddad, T. S.; Mylvaganam, M.; McConville, D. H.; Rettig, S. J. *J. Am. Chem. Soc.* **1993**, *115*, 2782. (c) Cohen, J. D.; Mylvaganam, M.; Fryzuk, M. D.; Loehr, T. M. *J. Am. Chem. Soc.* **1994**, *116*, 9529. (d) Fryzuk, M. D.; Love, J. B.; Rettig, S. J. *Organometallics* **1998**, *17*, 846.

(11) Basch, H.; Musaev, D. G.; Morokuma, K.; Fryzuk, M. D.; Love, J. B.; Seidel, W. W.; Albinati, A.; Koetzle, T. F.; Klooster, W. T.; Mason, S. A.; Eckert, J. *J. Am. Chem. Soc.* **1999**, *121*, 523.

(12) Musaev, D. G.; Basch, H.; Morokuma, K. To be submitted for publication.

(13) (a) Bauschlicher, C. W., Jr.; Pettersson, L. G. M.; Siegbahn, P. E. M. *J. Chem. Phys.* **1987**, *87*, 2129. (b) Musaev, D. G. *Russ. J. Inorg. Chem.* **1988**, *33*, 3207. (c) Siegbahn, P. E. M. *J. Chem. Phys.* **1991**, *95*, 364. (d) Blomberg, M. R. A.; Siegbahn, P. E. M. *J. Am. Chem. Soc.* **1993**, *115*, 6908.

on each Zr atom are conserved, while H atoms replace the $-CH_2$, $-SiMe_2$, and phenyl groups. Since the coordinating P and N atoms are not connected in the $[p_2n_2]$ model as in the actual macrocyclic $[P_2N_2]$ ligand, the structurally more rigid aspect of the extended ligand is lost. In addition, the electronic and the steric effects of the substituents are lost in the model phosphine ligands. However, the primary electronic effects of phosphine and imine ligands are retained. As each NH_2 group formally accepts one electron from Zr atom and the bridging N_2 molecule accepts four more, each Zr is formally d^0 and the electronic ground state of the model complex is a closed shell singlet state. Triplet electronic states were not examined. We are presently extending the present study with the use of the real ligand $[P_2N_2]$ employing the IMOMM method, and the results will be published elsewhere.[14]

The electronic structure calculations were carried out with the hybrid density functional method B3LYP,[15] as implemented in the GAUSSIAN-94 package,[16] in conjunction with the Stevens−Basch−Krauss (SBK)[17] effective core potential (ECP) (a relativistic ECP for the Zr atom) and the standard 4-31G, CEP-31, and (8s8p6d/4s4p3d) basis sets for the H, (C, P, and N), and Zr atoms, respectively.

Preliminary calculations tested the effect of d-type polarization functions located on the bridging nitrogen atoms on the geometric parameters. Because the N_2 molecule in the complex is still expected to have partial multiple bond character, the d-type function could be needed. Full optimization of the equilibrium geometry of the complexes **1**, $[p_2n_2]Zr(\mu\text{-}\eta^2\text{-}N_2)Zr[p_2n_2]$, and **7**, $[p_2n_2]Zr(\mu\text{-}\eta^2\text{-}NNH)Zr[p_2n_2](\mu\text{-}H)$ (vide infra), with the d-polarization functions on the bridging nitrogen atoms (using a Gaussian exponent of 0.8) showed a calculated shortening of the bridging N−N distance by 0.12 and 0.07 Å, respectively, relative to the optimized geometry obtained without the d-type functions on the bridging N_2. The smaller effect in complex **7** is justified by its more saturated nature compared to **1** due to the protonation of one of the bridging nitrogen atoms. To be able to describe all the bonding forms of bridging N_2 on an equal footing, the d-type functions on these two nitrogen atoms were retained in all the calculations reported here. The effect of phosphorus atom d-type functions on the calculated $Zr-PH_3$ bond lengths of model complexes **1** and **7** was also tested; here the influence was found to be negligibly small and, therefore, d-type functions on the P atom were not included in further calculations.

However, computational studies[18] of the model $(H)_3ZrPR_3^+$ complex show that the stepwise substitution of R = H by R = Me steadily increased the $Zr-PR_3$ binding energy, which is consistent with experimental studies on the Rh and Ru complexes,[19] indicating a strengthening of the Zr−P bond. Thus, the simplification of using NH_2 and PH_3 in the model $[p_2n_2]$ ligand instead of the real macrocyclic $[P_2N_2]$ ligand is expected to result in weaker Zr−P bonds in all the geometric structures studied here. The more rigid macrocyclic structure of the real $[P_2N_2]$ ligand, together with the stronger Zr−N bonding, will not allow a substantial lengthening of the Zr−P bond distance. In the optimized geometric structure for complex **1** with the $[p_2n_2]$ ligand, the $Zr-PH_3$ distances were found to be calculated too large by ∼0.2 Å compared to experiment.[7] We could not put substituents on the phosphines, because this would put the size of the calculations beyond current capabilities. In some of our present calculations, the weaker Zr−P bond in the model complexes and its expected effect on the calculated Zr−P distances were compensated for by reoptimizing all the equilibrium geometries of the complexes studied here using a fixed Zr−P bond distance of 2.80 Å. This procedure is intended to simulate the constraints of the macrocyclic ligand and their results will be discussed and interpreted alongside the unconstrained results. The external NH_2 groups (formally as NH_2^-) are expected to be more strongly bound to Zr than PH_3 by the electrostatic interaction, and d-type functions were not used on these N atoms. The calculated $Zr-NH_2$ distances in the model complex are much closer to the X-ray results for **1** than the Zr−P distances.

Geometries of the reactant, intermediates, transition states (TSs), and products of the reaction $[p_2n_2]Zr(\mu\text{-}\eta^2\text{-}N_2)Zr[p_2n_2]$ (**1**) + H_2 were determined by gradient optimization. Since the systems studied here were too large for the local computer resources, it was not possible to carry out second-derivative calculations. To confirm the nature of the calculated TS, quasi-IRC (intrinsic reaction coordinate) calculations were carried out in the following manner. For one direction, the TS geometry (optimized but with a small residual gradient) was simply released for direct equilibrium (Eq) geometry optimization. Once one Eq geometry is obtained, the other Eq geometry was obtained by stepping from the TS geometry in the reverse direction, as indicated by the eigenvector of the imaginary eigenvalue of the approximate Hessian, and releasing for equilibrium optimization. In this manner, the TS and Eq geometries in the reaction path were "connected". The energies given here and discussed below do not include zero-point energy correction (ZPC) or any other spectroscopic or thermodynamic terms.

3. Results and Discussion

All the calculated equilibrium structures and transition states on the potential energy surface of the reaction of **1** with H_2 are shown in Figure 1. The reaction potential energy profile is shown in Figure 2. Their Mulliken charges are tabulated in Table 1.

A. Structure of $Zr(N_2)Zr$ Complex 1. In general, reactant complex, **1**, which is calculated to have a bent Zr_2N_2 unit, could have various isomeric forms with regard to the arrangement of the NH_2 and PH_3 groups relative to the bridging N−N axis. In the optimized structure shown in Figure 1, the bridging N^1-N^2 axis (of the N_2 molecule) is *perpendicular* ($\phi = 90°$) to the ligand N−N axis (of the two NH_2 ligands attached to each Zr atom) but *parallel* to the P−P axis (of the two PH_3 ligands attached to each Zr atom). We have confirmed that this structure is energetically the most favorable under the D_{2h} constraint. Another structure with the bridging N−N *parallel* ($\phi = 0°$) to the ligand N−N and *perpendicular* to the P−P is calculated to be 18 kcal/mol higher. This result can be understood in terms of the larger repulsion in the latter complex between the negative charges of the nitrogen atoms in NH_2 (−0.83 e) and in the bridging N_2 atoms (−0.45 e), as shown in Table 1. An attempt to optimize a structure with the bridging N^1-N^2 axis initially bisecting the $N^{ligand}-Zr-P$ angles ($\phi = 45°$) reverted to structure **1** presented in Figure 1.

In the above-discussed isomers, the ligands of the same type are situated trans to each other: N trans to N and P trans to P, which is the conformation found experimentally with the $[P_2N_2]$ ligand. We have also calculated several possible isomers that may arise from the cis location of the same ligands. In these isomers, the bridging N−N axis can then bisect either the $N^{ligand}-Zr-P$ angles or the P−Zr−P angles, or align with a $N^{ligand}-Zr-P$ axis. In each case, structure **1** was found to be more stable. Thus, structure **1** represents the most stable coordinating ligand geometry with regard to the arrangement

(14) Yates, B.; Musaev, D. G.; Basch, H.; Morokuma, K. To be submitted for publication.

(15) (a) Becke, A. D. *J. Chem. Phys*. **1993**, *98*, 5648. (b) Lee, C.; Yang, W.; Parr, R. G. *Phys. Rev*. **1988**, *B37*, 785. (c) Stephens, P. J.; Devlin, F. J.; Chabalowski, C. F.; M. J. Frisch, M. J. *J. Phys. Chem*. **1994**, *98*, 11623.

(16) *Gaussian 94*, Frisch, M. J.; Trucks, G. W.; Schlegel, H. B.; Gill, P. M. W.; Johnson, B. G.; Robb, M. A.; Cheeseman, J. R.; Keith, T. A.; Petersson, J. A.; Montgomery, J. A.; Raghavachari, K.; Al-Laham, M. A.; Zakrzewski, V. G.; Ortiz, J. V.; Foresman, J. B.; Cioslowski, J.; Stefanov, B. B.; Nanayakkara, A.; Challacombe, M.; Peng, C. Y.; Ayala, P. Y.; Chen, W.; Wong, M. W.; Andres, J. L.; Replogle, E. S.; Gomperts, R.; Martin, R. L.; Fox, D. J.; Binkley, J. S.; DeFrees, D. J.; Baker, J.; Stewart, J. J. P.; Head-Gordon, M.; Gonzales, C.; Pople, J. A. Gaussian Inc.: Pittsburgh, PA, 1995.

(17) (a) Stevens, W. J.; Basch, H.; Krauss, M. *J. Chem. Phys*. **1984**, *81*, 6026. (b) Stevens, W. J.; Krauss, M.; Basch, H.; Jasien, P. G. *Can. J. Chem*. **1992**, *70*, 612.

(18) Musaev, D. G.; Basch, H.; Morokuma, K. Unpublished results.

(19) (a) Serron, S.; Nolan, S. P.; Moloy, K. G. *Organometallics* **1996**, *15*, 4301. (b) Serron, S.; Luo, L.; Stevens, E. D.; Nolan, S. P.; Jones, N. L.; Fagan, P. J. *Organometallics* **1996**, *15*, 5209.

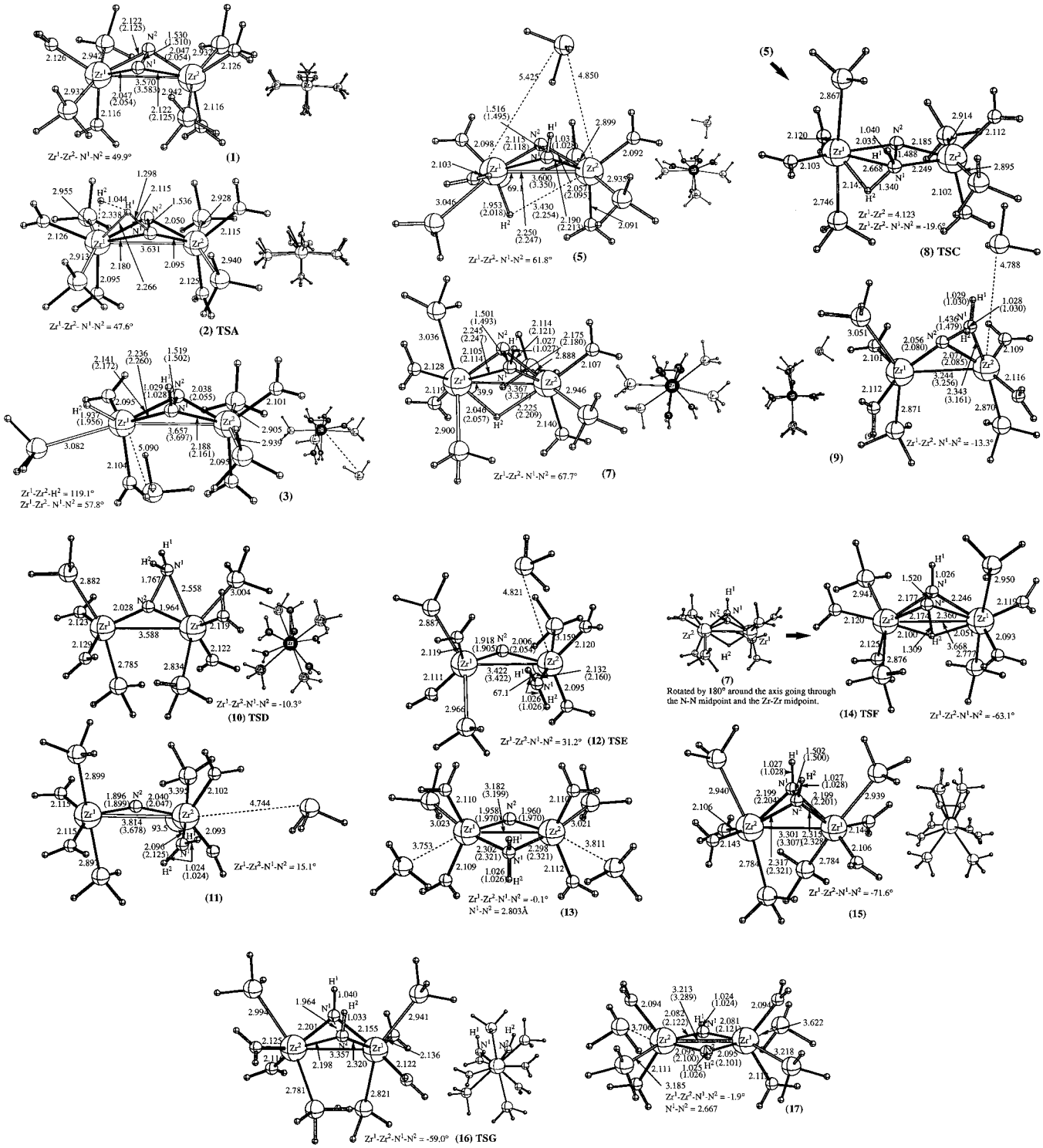

Figure 1. The calculated geometries (distances in Å and angles in deg) of the reactants, intermediates, transition states, and products of the reaction of $[p_2n_2]Zr(\mu\text{-}\eta^2\text{-}N_2)Zr[p_2n_2]$ with a hydrogen molecule. Numbers given in parentheses are calculated for with the constraint of $R(Zr-P) = 2.80$ Å.

of the external NH_2 and PH_3 ligands around each Zr atom, which is in accord with the experiment.

As noted above, **1** is calculated to have a bent Zr_2N_2 configuration, hinged at the N−N axis, and 24.4 kcal/mol more stable than the planar Zr_2N_2 in D_{2h} symmetry. This result is contrary to the earlier theoretical studies[13] on the naked Zr_2N_2, and to the experiment on **I**.[7] Note that the calculated bending, with the $Zr^1-Zr^2-N^1-N^2$ dihedral angle of 49.9° or the distance between the Zr^1-Zr^2 midpoint and the N^1-N^2 midpoint of 0.954 Å, is accompanied by a substantial reduction in the N^1-N^2 (1.698 Å in D_{2h} to 1.530 Å in **1**; 1.43 Å), $Zr-N^1$ (2.077 Å in D_{2h} to 2.047 Å in **1**; 2.01 Å), the largest Zr−P (3.016 Å in D_{2h} to 2.942 Å in **1**; 2.734 Å), and Zr−Zr (3.792 Å in D_{2h} to 3.570 Å in **1**; 3.756 Å) distances (where the third number in parentheses is from the X-ray crystal data for complex **I**[7]). The origin of the bend is probably electronic in nature, i.e., due to more extensive opportunities for orbital mixing between the Zr (4d, 5s, and 5p) and molecular nitrogen (σ, σ^*, π, π^*) valence electrons in the lower symmetry. It is, therefore, probable that the extended macrocyclic ligands prevent the bending in the

Table 1. Calculated Mulliken Charges (in e) of Selected Atoms and Groups of Various Structures[a]

atom	1	2	3	5
N^1	−0.45 (−0.44)	−0.50	−0.59 (−0.55)	-0.60 (−0.54)
N^2	−0.45 (−0.44)	−0.45	−0.47 (−0.47)	-0.49 (−0.40)
Zr^1	0.95 (0.83)	1.05	0.98 (0.79)	1.00 (0.89)
Zr^2	0.95 (0.83)	0.61	0.67 (0.59)	0.69 (0.48)
H^1	0	0.18	0.33 (0.34)	0.32 (0.31)
H^2	0	−0.11	−0.11 (−0.09)	−0.14 (−0.17)
N	−0.83 (−0.83)	−0.83	−0.84 (−0.81)	−0.82 (−0.80)
NH_2	−0.30 (−0.29)	−0.27	−0.28 (−0.27)	−0.27 (−0.26)
P	−0.03 (0.02)	−0.01	−0.01 (0.04)	−0.02 (0.04)
PH_3	0.05 (0.10)	0.08	0.07 (0.11)	0.07 (0.12)

atom	7	8	9	10	11	12
N^1	−0.56 (−0.54)	−0.48	−0.54 (−0.45)	−0.60	−0.90 (−0.88)	(−0.88)
N^2	−0.43 (−0.42)	−0.52	−0.60 (−0.63)	−0.61	−0.76 (−0.68)	(−0.64)
Zr^1	0.92 (0.80)	0.89	0.83 (0.71)	0.86	1.07 (0.75)	(0.75)
Zr^2	0.73 (0.58)	0.43	0.68 (0.64)	0.69	0.98 (0.85)	(0.80)
H^1	0.32 (0.32)	0.31	0.36 (0.26)	0.28	0.31 (0.31)	(0.31)
H^2	−0.14 (−0.13)	0.14	0.32 (0.27)	0.28	0.29 (0.30)	(0.31)
N	−0.81 (−0.80)	−0.82	−0.82 (−0.82)	−0.82	−0.85 (−0.81)	(−0.80)
NH_2	−0.27 (−0.26)	−0.28	−0.29 (−0.28)	−0.28	−0.30 (−0.27)	(−0.26)
P	−0.01 (0.04)	0.03	−0.03 (0.03)	0.00	−0.02 (0.03)	(0.03)
PH_3	0.06 (0.11)	0.09	0.02 (0.08)	0.05	0.05 (0.11)	(0.10)

atom	13	14	15	16	17
N^1	−0.95 (−0.92)	−0.59	−0.59 (−0.58)	−0.68	−0.94 (−0.90)
N^2	−0.65 (−0.62)	−0.39	−0.59 (−0.58)	−0.58	−0.94 (−0.90)
Zr^1	1.09 (0.80)	0.83	0.79 (0.73)	0.64	1.31 (0.99)
Zr^2	1.08 (0.80)	0.52	0.79 (0.71)	0.90	1.32 (1.00)
H^1	0.34 (0.34)	0.32	0.29 (0.29)	0.30	0.31 (0.28)
H^2	0.34 (0.34)	0.08	0.29 (0.29)	0.28	0.30 (0.28)
N	−0.83 (−0.78)	−0.81	−0.81 (−0.80)	−0.81	−0.85 (−0.81)
NH_2	−0.29 (−0.25)	−0.27	−0.29 (−0.28)	−0.27	−0.29 (−0.26)
P	−0.08 (−0.01)	−0.01	0.06 (0.02)	0.05	−0.11 (0.00)
PH_3	−0.02 (0.07)	0.08	0.05 (0.07)	0.06	−0.05 (0.07)

[a] Numbers in parentheses are for the Zr−P constrained optimized geometries. N, NH_2, P, and PH_3 values are averages.

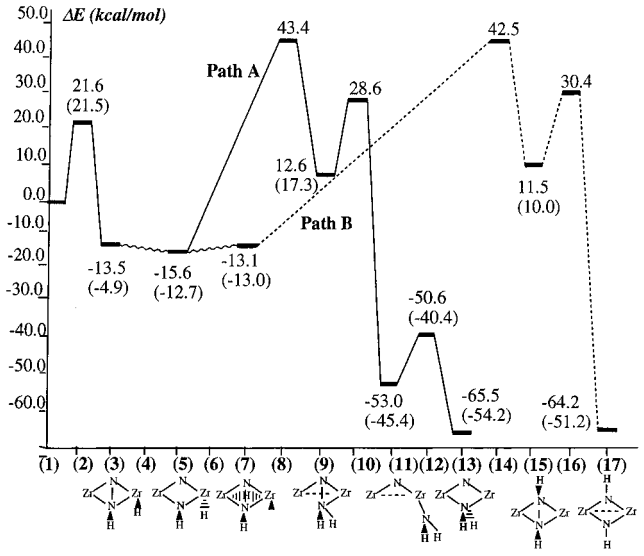

Figure 2. The calculated relative energies (in kcal/mol, relative to the reactants **1** + H_2) of the intermediates, transition states, and products of the reaction of complex **1** with a hydrogen molecule. Numbers given in parentheses are calculated with the constraint of R(Zr−P) = 2.80 Å.

real complex **I**. This point has been confirmed by IMOMM calculations[14] on the real complex **I**; these calculations show that the Zr−NN−Zr core is nearly planar for the real complex **I**, which is consistent with experimental findings. One notices in Figure 1 that the N−N distance in **1** is 1.530 Å, corresponding to a single N−N bond. In **1**, the two π-bonds in the molecular nitrogen are completely broken, and the Zr−NN−Zr core can be considered as a metallabicycle.

B. H_2 Activation with Complex 1. The first step of the reaction of **1** with a H_2 molecule is the coordination of dihydrogen to **1**. As shown in our previous paper,[11] this coordination does not produce the dihydrogen complex (H_2)·**1**, but leads directly to the activation of the H−H bond via the transition state TSA, structure **2** in Figure 1, to the diazenidohydride complex [p_2n_2]Zr(μ-η^2-N_2H)Zr[p_2p_2](μ-H), **3**. This is a four-center transition state for addition of H_2 to two centers, Zr^1 and N^1, where the H^1−H^2 bond is broken and at the same time the terminal Zr^1−H^2 and the N^1−H^1 bonds are formed. The bond distance changes in the Zr_2N_2 core region from **1** to **3** are as expected for an addition reaction; Zr^1−N^2 and Zr^2−N^2 bond lengths do not change significantly, while Zr^1−N^1 increased by 0.13 Å and Zr^2−N^1 decreased by 0.03 Å due to the increased coordination of Zr^1 and N^1. The N^1−N^2 bond distance would also be expected to become larger, but the actual change is found to be insignificant. In **3**, the H^1 atom in the N^1−H^1 bond becomes positively charged (by +0.33 e) while H^2 in the Zr^1−H^2 bond becomes negatively charged, and the charges are also drawn from the external ligands to the Zr^1 center.

The barrier height for the oxidative addition of H_2 to **1** at TSA **2** is calculated to be 21.6 kcal/mol. The activation barrier changed very little between the fully optimized calculation and the Zr−P constrained optimization (21.5 kcal/mol). The actual barrier will probably be lower when zero-point energy differences are taken into account between **1** + H_2 and **3**. The tunneling abilities of the hydrogen atom should also be taken

into account in this context. The result of all these corrections could be an effective barrier that is smaller than the calculated value.

The product of the reaction, complex **3**, is calculated to be 13.5 and 4.9 kcal/mol exothermic relative to reactants, in the unrestricted and the Zr−P constrained geometries, respectively. The higher energy (lower stability) of the latter comes from the tendency of the two Zr^1-P bonds to lengthen considerably in the unconstrained geometry to make room for the new Zr^1-H^2 bond. The latter bond is broken because of its eclipsed alignment with the N^1-H^1 bond and the higher coordination number (>6) on Zr^1. This repulsion, in turn, pushes the weakly bound phosphine groups on the same Zr atom to large, essentially dissociated Zr−P distances. The almost free motion of the phosphine groups is inconsistent with the constrained geometric structure of the real, strongly bound macrocyclic $[P_2N_2]$ ligand, which will restrict the freedom of motion of the (substituted) phosphine groups. Therefore, the 4.9 kcal/mol stability of the constrained **3** geometry is probably the more realistic value. It should be noted that the calculated Zr−P distances in TSA, **2**, are very similar to those in **1**, so that the calculated barrier height will not be raised by constraining the Zr−P distances in TSA, relative to **1** + H_2. In accord with its mode of formation, **3** has the N^1-H^1 and Zr^1-H^2 bonds aligned almost parallel and protruding from the same "face" of the Zr_2N_2 core.

C. Transformation of Diazenidohydride Complex 3. The diazenidohydride complex **3**, which has the N−H and Zr−H bonds oriented parallel or on the same face of the Zr_2N_2 core, can rearrange into other conformation isomers. We have found structure **5** in Figure 1, with the N−H and Zr−H bonds antiparallel or on the opposite faces. In **5**, without constraint, Zr^1, which has the $Zr-H^2$ bond and is very crowded, loses one phosphine from the first coordination shell to the second coordination shell. With the Zr−P bond constraint, of course the phosphine is forced to stay in the first coordination shell. Interestingly, the interaction energy of this phosphine is weak either way, and does not have much effect on the overall energetics seen in Figure 2: **5** is 15.6 and 12.6 kcal/mol lower than reactants **1** + H_2 in the Zr−P unconstrained and constrained geometries, respectively. In other words, the **3** → **5** transformation is 2.1 and 7.7 kcal/mol exothermic at the Zr−P unconstrained and constraint geometries, respectively.

The search for a transition state for the **3** → **5** transformation is complicated. Besides the relative directions of Zr^1-H^2 and N^1-H^1 bonds, **3** and **5** differ by ∼90° in the relative orientations of the $[p_2n_2]$ ligands on different Zr atoms: **3** is N^1-H^1/Zr^1-H^2 parallel and $[p_2n_2]$ eclipsed, and **5** is N^1-H^1/Zr^1-H^2 antiparallel and $[p_2n_2]$ staggered. Recall that the eclipsed $[p_2n_2]$ comes from structure **1**, which was found to be the most stable conformation theoretically and experimentally. Structure **5** with the eclipsed $[p_2n_2]$ conformation (**5′**) is less stable then **5** itself, so both geometrical differences between **3** and **5** are real. Despite our several careful attempts, we could not find the TS separating **3** and **5**. For example, the attempt involving the stepwise twisting of the Zr^1-H^2 bond leads to a "transition state" with the very small negative eigenvalue, which lies only 9 kcal/mol higher than structure **3**. This can be taken as the upper limit of the barrier separating **3** and **5**. All attempts to search for the "real" transition state by optimizing all geometrical parameters failed and led to different minimum structures, **3**, **5**, **3′**, and **5′**, of which the last two are not presented in Figure 1. Therefore we have concluded that (i) the potential energy surface for the **3** → **5** transformation is most likely to be flat, (ii) the associated barrier is very likely to be low, and (iii) the flexibility of the arrangements of the individual NH_2 and PH_3 ligands about each Zr allows multiple minima.

Another equilibrium structure **7** was found, which had a bridging $Zr^1-H^2-Zr^2$ arrangement with longer Zr−H bond lengths (2.046, 2.225 Å) than the terminal Zr^1-H^2 bond, 1.95 Å, of structures **3** and **5**. The $Zr^2-H^2-Zr^1$ bridging structure **7** can be identified with the species observed experimentally in solution. In the unconstrained geometries, 7 is less stable than 5 by 2.5 kcal/mol and than **3** by 0.4 kcal/mol. The energy barrier between **5** and **7** is expected to be very small and was not calculated. For a simplified model complex,[18] $Cl_2Zr(\mu\text{-}\eta^2\text{-}N_2H)(\mu\text{-}H)ZrCl_2$, we found this barrier to be less than 1 kcal/mol.

In the Zr−P constrained optimizations, however, the two structures, **5** and **7**, essentially merge to the very similar bridging geometry. As seen in Figure 1, a large decrease occurs in the Zr^2-H^2 distance in **5** from 3.430 (unconstrained) to 2.254 Å (Zr−P constrained) and converges to a structure that resembles **7**. Now structures **7** and **5** are nearly degenerate; the latter lies only 0.4 kcal/mol higher than the former. Therefore, in the more realistic Zr−P constrained optimizations, structures **5** and **7** can be considered to be a single diazenidohydride structure, the H-bridged $[p_2n_2]Zr(\mu\text{-}\eta^2\text{-}NNH)Zr[p_2n_2](\mu\text{-}H)$ structure **7**, which agrees with the experimental finding. Structure **5** is an artifact of our unconstrained model system; one of the phosphine ligands dissociated from Zr to make space for the terminal Zr^1-H^2 bond.

If we compare the H-bridged **7** directly to the H-terminal **3**, we see the expected contraction of the Zr^1-Zr^2 distance due to the bridging $Zr^1-H^2-Zr^2$ bond which will act to hold the Zr metal atoms about 0.30 Å closer in **7** than in **3**. The stronger Zr−Zr interaction would be expected to weaken and lengthen the $Zr-N^1/N^2$ bonds, but the shorter Zr−Zr distance should also act to squeeze these Zr−N distances to smaller values. The two opposing effects seem to cancel and there are no consistent trends in these Zr−N bond lengths in going from **3** to **7**.

D. Migration of H from Zr to N and Cleavage of the N−N Bond. From the H-bridged $[p_2n_2]Zr(\mu\text{-}\eta^2\text{-}NNH)Zr[p_2n_2](\mu\text{-}H)$ structure **7** (or **5**), we have found that the reaction splits into two distinct branches of hydride migration, both leading to the formation of the second N−H bond and the loss of the Zr−H−Zr (or Zr−H) bond. One branch, which we call path **A**, starts from **5** and proceeds through the H^2 migration transition state, TSC **8**, to reach a hydrazono (NH_2-N) intermediate **9**. This is then followed by the N−N bond fission via TSD. The overall pathway for path **A** is **5** → TSC **8** → **9** → TSD **10** → **11** → TSE **12** → **13**. The final structure **13** has a completely severed N^1-N^2 bond (2.80 Å) where an N^1H_2 group and a bare N^2 atom are bridging the two Zr atoms in a symmetric geometry. The second branch, path **B**, involves migration of the bridging ($Zr^1-H^2-Zr^2$) hydrogen atom in **7** to the nitrogen atom N^2 that did not carry a hydrogen atom and proceeds through a hydrado (NH−NH) intermediate through the following route: **7** → TSF **14** → **15** → TSG **16** → **17**. The N^1-N^2 bond preserved (1.50 Å) in **7** is broken (2.67 Å) in the final structure **17**, giving a planar $Zr_2(NH)_2$ arrangement. The sequence of equilibrium structures and transition states, as well as their connectivity from **7** (or **5**) to **13** and from **7** to **17**, was obtained as described in Section 2.

Path **A** is characterized by a high initial barrier of about 60 kcal/mol at TSC **8** and a very exothermic (−65.5 kcal/mol) terminal point $[p_2n_2]Zr(\mu\text{-}NH_2)(\mu\text{-}N)Zr[p_2n_2]$, **13**. In **9** the NH_2 unit is already fully formed and the Zr^1-N^1 bond has been broken. The Zr^2-N^1 bond remains, but at the expense of ejecting a proximate phosphine group out to ∼4.8 Å. In the Zr−P

constrained optimized structure for **9**, however, the Zr^2-N^1 bond is broken, leaving a protruding NH_2 group attached only to the bridging N^2 atom. In the next step along this reaction path, the N^2-N^1 bond cleavage takes place at TSD **10**, leading to the intermediate **11**. In **11**, N^2 is located at the bridging position between two Zr atoms, while the newly formed N^1H_2 fragment moved completely to one of the Zr atoms, Zr^2. As a result the Zr^1-N^2 bond (1.90 Å) becomes shorter by 0.14 Å than the Zr^2-N^2 bond (2.04 Å). Later, the N^1H_2 group migrates from Zr^2, in structure **11**, via TSE **12** to the bridging position between two Zr atoms, leading to the formation of the N^1-Zr^1 bond in **13**. Thus, the sequence of TS and equilibrium structures that takes **5** to **13** is a roundabout reaction path involving a sequence of four equilibrium and three transition state structures. The least motion, direct formation of **13** from **5** via a TSC-like structure, does not happen. The energy of TSC is already sufficiently high so as to effectively block this path. To go directly to **13** would also require the incipient breaking of the molecular N−N bond to give an even higher saddle point energy. The actual sequence of equilibrium and transition state structures of path **A** apparently allows this bond breaking energy to be absorbed by other processes so that this reaction path is a cascade of energetically more stable structures (**9** → **11** → **13**) and decreasing barrier heights (TSD, TSE) from TSD to **13**. The conclusions from this path are that the direct migration of the bridging hydrogen atom to a bridging NH has a high reaction barrier, which will be even higher if the N^1-N^2 bond is also broken in the process, even if the rupture eventually leads to a more stable structure.

Path **B** which leads from **7** to **17** has only two transition states (TSF **14** and TSG **16**) and one intermediate equilibrium structure **15**. As with path **A**, this reaction path involves the migration of H^2 from Zr^1 to N^2 to form the metastable **15** structure, where the N^1-N^2 bond length is essentially unchanged at ∼1.50 Å. The bridging nitrogen atoms in **15** are effectively four-coordinate with the N−N bond still in place. The final step to reach the very stable **17** structure is to stretch the N−N bond from 1.502 Å in **15** through 1.964 Å (in TSG **16**) to the completely broken 2.667 Å in **17**. In this latter step the bent Zr_2N_2 core and the N−H bonds aligned almost perpendicular to the N−N axis, which were preserved in **15** → **16**, are dramatically changed, and the $Zr_2(NH)_2$ core is now completely planar with near D_{2h} symmetry. Another dramatic geometry change worthy of mention is the rotation of the incipient N^2-H^2 bond in TSF **14** from being antiparallel to the existing N^1-H^1 bond (across N−N) to the parallel conformation in **15**. This spontaneous rearrangement is apparently caused by the H^2 atom internal to the Zr_2N_2 bond being squeezed out by steric effects to the more stable external N−H position, even though this gives eclipsed N−H bonds in **15**. As a paradigm, this barrierless rearrangement means that adding a H atom to a bridging N atom could come from a backside attack under the proper conditions. Finally, as in channel **A**, the large (45.6 kcal/mol) initial barrier for channel **B** precludes this reaction path from reactively adding a H atom to the bare N atom to form **15**, despite the large exothermicity (−51.1 kcal/mol) for **17** relative to **7**.

The most important feature of the first step in both paths **A** and **B** is the very large (56−59 kcal/mol) barrier height, even though the end products are 64−65 kcal/mol more stable than reactants **1** + H_2 or 50−51 kcal/mol more stable than **5** and **7**. These high barriers prevent the reaction from proceeding to form products with the second N−H bond, either on the same bridging nitrogen atom with the first N−H bond or on the second, "bare" bridging nitrogen. Thus, the dinitrogen complex $[p_2n_2]Zr(\mu\text{-}\eta^2\text{-NNH})Zr[p_2n_2](\mu\text{-H})$, **7**, is the only product of the reaction of one molecule of H_2 with dinitrogen complex $[p_2n_2]Zr(\mu\text{-}\eta^2\text{-}N_2)Zr[p_2n_2]$, **1**.

4. Conclusions

Above we have presented the theoretically derived mechanism of the reaction of binuclear zirconium dinitrogen complex $[p_2n_2]Zr(\mu\text{-}\eta^2\text{-}N_2)Zr[p_2n_2]$ (**1**, where $p_2n_2 = (PH_3)_2(NH_2)_2$ is a model of the experimentally studied P_2N_2 = PhP($CH_2SiMe_2NSiMe_2CH_2)_2$PPh) with a hydrogen molecule. It has been shown that this reaction proceeds via (i) the activation of H−H σ-bond via a "metathesis-like" transition state where simultaneously Zr−H and N−H bonds are formed and the H−H and one of the N−N π-bonds are broken, to produce diazenidohydride complex **3**, $[p_2n_2]Zr(\mu\text{-}\eta^2\text{-NNH})Zr(H)[p_2n_2]$, and (ii) migration of the Zr-bonded hydride ligand to a position bridging the two Zr atoms to form diazenido−μ-hydride complex **7**, $[p_2n_2]Zr(\mu\text{-}\eta^2\text{-NNH})Zr[p_2n_2](\mu\text{-H})$. The entire reaction is calculated to be exothermic by 13−15 kcal/mol. The rate-determining step of this reaction is found to be the activation of the H−H bond, which occurs with a 21-kcal/mol barrier.

The diazenido−μ-hydride complex $[p_2n_2]Zr(\mu\text{-}\eta^2\text{-NNH})Zr[p_2n_2](\mu\text{-H})$, **7**, with only one N−H bond, which experimentally was observed in solution, is not the lowest energy structure in the potential surface. Complexes $[p_2n_2]Zr(\mu\text{-NNH}_2)Zr[p_2n_2]$ (**13**, with a bridging NH_2) and $[p_2n_2]Zr(\mu\text{-NHNH})Zr[p_2n_2]$ (**17**, with two N−H units) are calculated to be more stable than the diazenido−μ-hydride complex **7** by about 50 kcal/mol. However, these complexes cannot be generated from the **1** + H_2 reaction at ambient laboratory conditions because there exist very high (nearly 60 kcal/mol) barriers separating them from **7**.

We have not examined alternative reaction paths involving low-lying triplet excited states. Considering the fact that the intermediates in this reaction are nearly coordinatively saturated, it is not very likely that the triplet states play an important role.

In the present study we adopted model ligands, $[p_2n_2] = (PH_3)_2(NH_2)_2$, in place of the real ligands $[P_2N_2]$ = PhP($CH_2SiMe_2NSiMe_2CH_2)_2$PPh used in the experiment. In structures **3**, **5**, **9**, **11**, **12**, and **13** we found that one of the Zr−PH_3 bonds is almost dissociate and a phosphine ligand PH_3 tends to escape from the first coordination shell to reduce the strain from overcrowding at the metal center. This would not easily take place with the real chelating ligands. To mimic this situation with our model $[p_2n_2]$, we also used the Zr−P constrained calculations, in which the Zr−P distance in the $[p_2n_2]$ model system was constrained at 2.80 Å. Of course, this Zr−P constrained calculation is oversimplified. It is highly desirable to reexamine the present results by using the real ligand $[P_2N_2]$. The straightforward MO calculation for the real system is beyond the capacity of present computers. However, the ONIOM method[20] may be adopted, in which the most important part (reactive region) of the real system is handled with a high level of theory (in the present example, B3LYP), while the less important parts are handled with lower levels (such as semiempirical MO or molecular mechanics (MM)). Such a study is in progress and will be reported in the future.[14]

(20) (a) Maseras, F.; Morokuma, K. *J. Comput. Chem.* **1996**, *16*, 1170. (b) Matsubara, T.; Maseras, F.; Koga, N.; Morokuma, K. *J. Phys. Chem.* **1996**, *100*, 2573. (c) Humbel, S.; Sieber, S.; Morokuma, K. *J. Chem. Phys.* **1996**, *105*, 1959. (d) Svensson, M.; Humbel, S.; Morokuma, K. *J. Chem. Phys.* **1996**, *105*, 3654. (e) Matsubara, T.; Sieber, S.; Morokuma, K. *Int. J. Quantum Chem.* **1996**, *60*, 1101. (f) Froese, R. D. J.; Morokuma, K. *Chem. Phys. Lett.* **1996**, *263*, 393. (g) Svensson, M.; Humbel, S.; Froese, R. D. J.; Matsubara, T.; Sieber, S.; Morokuma, K. *J. Phys. Chem.* **1996**, *100*, 19357. (h) Froese, R. D. J.; Humbel, S.; Svensson, M.; Morokuma, K. *J. Phys. Chem.* **1997**, *101*, 227.

A very interesting question is whether and how easily $[p_2n_2]$-$Zr(\mu\text{-}\eta^2\text{-}NNH)Zr[p_2n_2](\mu\text{-}H)$, **7**, the product of the present reaction of **1** with one dihydrogen, reacts with the second (or more) H_2 molecule. A computational study of such reactions is in progress in our laboratory and will be reported shortly.[12]

Acknowledgment. The authors are grateful to Professor Michael D. Fryzuk for very stimulating discussions. H.B. acknowledges the Visiting Fellowship from the Emerson Center. The present research is in part supported by a grant (CHE-9627775) from the National Science Foundation. Acknowledgment is also made for generous support of computing time at Bar Ilan University Computer Center, Emerson Center of Emory University, US National Center for Supercomputing Applications (NCSA), and Maui High Performance Computer Center (MHPCC).

JA984408W